

Article

Static and Dynamic Analysis of Linear Piezoelectric Structures Using Higher Order Shear Deformation Theories

Konstantinos I. Ntaflos ¹, Konstantinos G. Beltsios ^{2,*} and Evangelos P. Hadjigeorgiou ^{1,*}¹ Department of Materials Science and Engineering, University of Ioannina, 45110 Ioannina, Greece² School of Chemical Engineering, National Technical University of Athens, Zografou, 15780 Athens, Greece

* Correspondence: kgbelt@mail.ntua.gr (K.G.B.); ehadjig@uoi.gr (E.P.H.)

Abstract: This paper explores the effects of shear deformation on piezoelectric materials and structures that often serve as substrate layers of multilayer composite sensors and actuators. Based on higher-order shear elastic deformation and electric potential distribution theories, a general mathematical model is derived. Governing equations and the associated boundary conditions for a piezoelectric beam are developed using a generalized Hamilton's principle. The static and dynamic behavior of the piezoelectric structure is investigated. A bending problem in static analysis and a free vibration problem in dynamic analysis are solved. The obtained results are in very good agreement with the results of the exact two dimensional solution available in the literature.

Keywords: piezoelectric beams; higher-order shear deformation theories; shear effects; Hamilton's principle; functional layers for composite sensors and actuators

1. Introduction

Elastic beams and plates are common structural elements in various structures. Piezoelectric beams and plates in the field of composite materials are of particular interest for their functional role in layered-composite sensors and actuators [1,2]. The more accurate way to analyze the mechanical properties of elastic beams and plates and study their response to different mechanical loads is using the three-dimensional mathematical theory of elasticity. Because of the complexity of the three-dimensional theory, the calculation and evaluation of static and dynamic characteristics is frequently attempted via the application of various simplified theories, described collectively as “technical or engineering theories” [3]. Nevertheless, it is well known that the elementary beam theory (ETB) in bending problems underestimates deflections and overestimates natural frequencies since it disregards the transverse shear deformation effect. Timoshenko [4] was the first to include refined effects such as rotatory inertia and shear deformation in the beam theory. This theory is widely referred to as Timoshenko beam theory (TBT) or first order shear deformation theory (FSDT).

The limitations of elementary theory of beam (ETB) and first order shear deformation theory (FSDT) led to the development of higher order shear deformation theories. There are many higher-order shear deformation theories available in the literature for static and dynamic analysis of elastic beams [5–11]. Ambartsumian [12] developed a bending theory of anisotropic plates and shallow shells. Kruszewski [13] studied the effect of transverse shear and rotary inertia on the natural frequency of a uniform beam. Reddy [14] has developed the well-known third-order shear deformation theory for the nonlinear analysis of plates with moderate thickness. The trigonometric shear deformation theories are presented by Touratier [15], Vlazov and Leontiev [3] and Stein [16] for thick beams. Soldatos [17] has developed hyperbolic shear deformation theory for homogeneous monoclinic plates. Karama et al. [18] studied the mechanical behavior of laminated composite beams by the new multi-layered laminated composite structures model with transverse



Citation: Ntaflos, K.I.; Beltsios, K.G.; Hadjigeorgiou, E.P. Static and Dynamic Analysis of Linear Piezoelectric Structures Using Higher Order Shear Deformation Theories. *J. Compos. Sci.* **2023**, *7*, 87. <https://doi.org/10.3390/jcs7020087>

Academic Editor: Francesco Tornabene

Received: 22 December 2022

Revised: 30 January 2023

Accepted: 14 February 2023

Published: 17 February 2023



Copyright: © 2023 by the authors. Licensee MDPI, Basel, Switzerland. This article is an open access article distributed under the terms and conditions of the Creative Commons Attribution (CC BY) license (<https://creativecommons.org/licenses/by/4.0/>).

shear stress continuity. Sayyad [19,20] has carried out a comparison of various linear shear deformation theories for the free vibration analysis of thick isotropic beams. Study of the literature [9,10,19,21,22] indicates that the research work dealing with bending analysis of thick elastic beams using higher-order shear deformation theories is still in its early stage. Furthermore, although various technical theories for piezoelectric beams can be found in the literature [1,2,23–26], no systematic derivation of higher-order theories for static and dynamic analysis of piezoelectric beams is available.

In the present study, a systematic derivation of a general mathematical model for static and dynamic analysis of piezoelectric beams is presented; the model is based on higher-order shear elastic deformation and electric potential distribution theories. Using a generalized Hamilton’s Principle [25,27] suitable for piezoelectric materials, the full set of equations of motion as well as the associated boundary conditions are determined for bending problems. Using this model, bending deflections (transverse displacement, rotation and electric potential) and natural frequencies (flexural and thickness shear mode frequencies) of a simply supported piezoelectric beam are calculated and compared with the results obtained using a two-dimensional model available in the relevant literature [28]. The obtained results are of practical importance for the more accurate design of layered-composite piezoelectric sensors and actuators in engineering applications.

More specifically, the form of the unified displacement field and unified electric potential field, and the strain–displacement and stress–strain relations, are presented in Section 2. The generalized Hamilton’s principle for the piezoelectric beam is described analytically and the full set of equations of motion and associated boundary conditions are determined for bending problems in Section 3. The bending problem of a simply supported piezoelectric beam under transverse loads is solved in Section 4, while the corresponding free flexural vibration problem is solved in Section 5. Various numerical results and related diagrams are presented and discussed in Section 6. Potential applications and future work of immediate interest is discussed briefly in Section 7.

2. Unified Theoretical Formulation for the Piezoelectric Beam

Considering a piezoelectric ceramic beam as shown in Figure 1, any boundary and transverse loading conditions might apply. The beam under consideration occupies the region given by the following:

$$0 \leq x \leq L, \quad -b/2 \leq y \leq b/2, \quad -h/2 \leq z \leq h/2,$$

where x, y and z are Cartesian co-ordinates, L is the length, h the thickness and b the width of the piezoelectric beam. The piezoelectric beam is subjected to transverse load of intensity $q(x)$ per unit length of the beam.

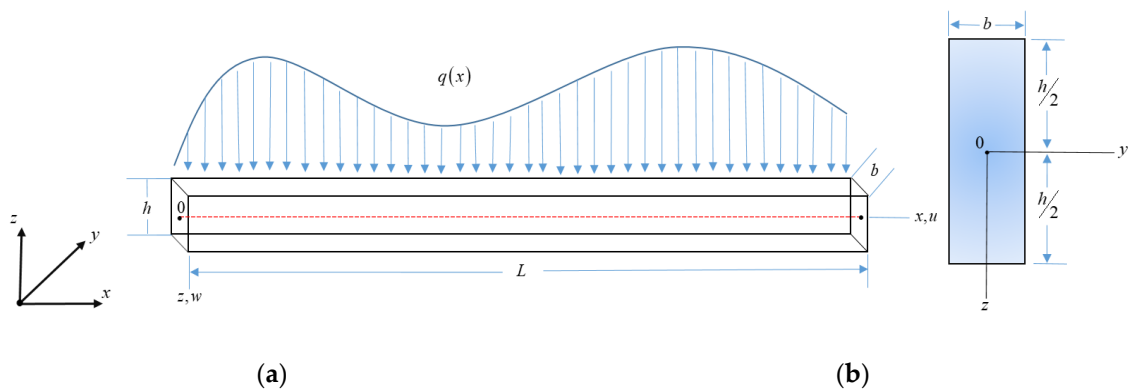


Figure 1. (a) Piezoelectric beam under bending in $x - z$ plane; (b) Cross-section of beam in $y - z$ plane.

2.1. The Displacement Field and Electric Potential

Based on the aforementioned assumptions, the displacement field [19] and the electric potential of the piezoelectric beam are given as below:

$$u(x, y, z, t) = -z \frac{\partial w(x, t)}{\partial x} + f(z)\varphi(x, t), \tag{1}$$

$$v(x, y, z, t) = 0, \tag{2}$$

$$w(x, y, z, t) = w(x, t), \tag{3}$$

$$\tilde{\varphi}(x, y, z, t) = g(z)\bar{\varphi}(x, t). \tag{4}$$

Here, u and w are the axial and transverse displacements of the beam center line in x and z directions, respectively, $\tilde{\varphi}$ is the electric potential and t is the time. Symbol φ represents the rotation of the cross-section of the beam at neutral axis, which is an unknown function to be determined. The functions $f(z)$, according to the shear stress distribution through the thickness of the beam, are given in Table 1.

Table 1. Function $f(z)$ for different high order shear stress distribution.

Model	Function $f(z)$
Ambartsumian (1958) [12]	$f(z) = \frac{z}{2} \left(\frac{h^2}{4} - \frac{z^2}{3} \right)$
Kruszewski (1949) [13]	$f(z) = \frac{5z}{4} \left(1 - \frac{4z^2}{3h^2} \right)$
Reddy (1990) [14]	$f(z) = z \left[1 - \frac{4}{3} \left(\frac{z}{h} \right)^2 \right]$
Touratier (1991) [15]	$f(z) = \frac{h}{\pi} \sin \frac{\pi z}{h}$
Soldatos (1992) [17]	$f(z) = z \cosh \left(\frac{1}{2} \right) - h \sinh \left(\frac{z}{h} \right)$
Karama et al. (2003) [18]	$f(z) = z \exp \left[-2 \left(\frac{z}{h} \right)^2 \right]$

The functions $g(z)$ describe the distribution of the electric potential inside the piezoelectric beam. According to the literature [18,21,23,24,26,29], various forms for $g(z)$ are given in Table 2. The form of the function $g(z)$ depends on the type of circuit conditions chosen for various applications. TYPE I refers to open circuit conditions and TYPE II refers to short circuit conditions.

Table 2. Function $g(z)$ describes the distribution of the electric potential along the thickness direction of the piezoelectric beam.

Circuit Conditions	Function $g(z)$	Author
TYPE I	$g(z) = -\frac{z}{h}$	Goldschmidtboeing and Woias (2008) [21]
TYPE I	$g(z) = \frac{2z}{h}$	Komeili et al. (2011) [30]
TYPE II	$g(z) = \frac{h}{\pi} \cos \left(\frac{\pi z}{h} \right)$	Fernandes and Pouget (2001) [29]
TYPE II	$g(z) = 1 - \left(\frac{2z}{h} \right)^2$	Wang et al. (2001) [26]
TYPE II	$g(z) = \cos \left(\frac{\pi z}{h} \right)$	Baroudi et al. (2018) [23]

The shear deformation effects are more important in thick beams than in slender beams. These effects are neglected in elementary bending theory of beams (Euler–Bernoulli Theory). To describe the correct bending behavior of thick beams including shear deformation effects, high order shear deformation theories are required. This can be achieved by the selection of proper kinematics and constitutive models.

The function $f(z)$ is included in the displacement field of high order theories to consider the effect of transverse shear deformation and achieve zero shear stress at the top and bottom surface of the beam [19].

2.2. Strain–Displacement and Stress–Strain Relations

Normal strain ϵ_x and transverse shear strain γ_{xz} for a linear piezoelectric beam are given by the following:

$$\epsilon_x = \frac{\partial u}{\partial x} = -z \frac{\partial^2 w}{\partial x^2} + f(z) \frac{\partial \varphi}{\partial x}, \tag{5}$$

$$\gamma_{xz} = \frac{\partial u}{\partial z} + \frac{\partial w}{\partial x} = f'(z) \varphi(x, t). \tag{6}$$

Axial stress (normal bending stress) σ_x , transverse shear stress τ_{xz} and electric displacement components D_x and D_z for the piezoelectric beam [25,27] are given by the following:

$$\sigma_x = \tilde{c}_{11} \epsilon_x - \tilde{e}_{31} E_z, \tag{7}$$

$$\tau_{xz} = c_{55} \gamma_{xz} - e_{15} E_x, \tag{8}$$

$$D_x = e_{15} \gamma_{xz} + \epsilon_{11} E_x, \tag{9}$$

$$D_z = \tilde{e}_{31} \epsilon_x + \tilde{\epsilon}_{33} E_z, \tag{10}$$

where \tilde{c}_{11} , \tilde{e}_{31} and $\tilde{\epsilon}_{33}$ are the reduced elastic, piezoelectric and dielectric constants under plane stress assumption from the 3-D constitutive relationship [26,31]; the latter constants are given by the following:

$$\begin{aligned} \tilde{c}_{11} &= \bar{c}_{11} - \frac{\bar{c}_{13}^2}{\bar{c}_{33}}, & \tilde{e}_{31} &= \bar{e}_{31} - \frac{\bar{c}_{13} \bar{e}_{33}}{\bar{c}_{33}}, & \tilde{\epsilon}_{33} &= \bar{\epsilon}_{33} + \frac{\bar{e}_{33}^2}{\bar{c}_{33}} \\ \bar{c}_{11} &= c_{11} - \frac{c_{12}^2}{c_{22}}, & \bar{c}_{13} &= c_{13} - \frac{c_{12} c_{23}}{c_{22}}, & \bar{c}_{33} &= c_{33} - \frac{c_{23}^2}{c_{22}} \\ \bar{e}_{31} &= e_{31} - \frac{c_{12} e_{32}}{c_{22}}, & \bar{e}_{33} &= e_{33} - \frac{c_{23} e_{32}}{c_{22}}, & \bar{\epsilon}_{33} &= \epsilon_{33} + \frac{e_{32}^2}{c_{22}}. \end{aligned} \tag{11}$$

Generally, the electric field vector for the piezoelectric beam in the quasi-electrostatic approximation is defined as follows:

$$E_i = -\frac{\partial \tilde{\varphi}}{\partial x_i}. \tag{12}$$

Thus, using Equation (4), the components of the electric field in the beam across x , y and z directions are given by the following:

$$\begin{aligned} E_x &= -\frac{\partial \tilde{\varphi}}{\partial x} = -g(z) \frac{\partial \bar{\varphi}}{\partial x}, \\ E_y &= -\frac{\partial \tilde{\varphi}}{\partial y} = 0, \end{aligned} \tag{13}$$

$$E_z = -\frac{\partial \tilde{\varphi}}{\partial z} = \frac{\partial g(z)}{\partial z} \bar{\varphi}(x, t) = -g'(z) \bar{\varphi}(x, t).$$

3. Governing Equations and Boundary Conditions

Using Equations (5) through (13) and Hamilton’s principle, variationally consistent governing differential equations and boundary conditions for the piezoelectric beam under consideration can be obtained.

The generalized form of the Hamilton’s principle for the piezoelectric beam (see also reference [25] for more details) is given as follows:

$$\delta \int_{t=t_1}^{t=t_2} (T - H_e + W_e) dt = 0, \tag{14}$$

where

$$\delta \int_{t=t_1}^{t=t_2} (T) dt = \delta \int_{t=t_1}^{t=t_2} \left[\frac{1}{2} \int_V \rho \{\dot{u}\}^T \{\dot{u}\} dV \right] dt, \tag{15}$$

$$\delta \int_{t=t_1}^{t=t_2} (-H_e) dt = -\delta \int_{t=t_1}^{t=t_2} \int_V \left(\frac{1}{2} \{\varepsilon\}^T [C] \{\varepsilon\} - \{\varepsilon\}^T [e]^T \{E\} - \frac{1}{2} \{E\}^T [\varepsilon] \{E\} \right) dV dt, \tag{16}$$

$$\delta \int_{t=t_1}^{t=t_2} (W_e) dt = \delta \int_{t=t_1}^{t=t_2} \int_{x=0}^{x=L} q w(x, t) dx dt = \int_{t=t_1}^{t=t_2} \int_{x=0}^{x=L} q (\delta w) dx dt, \tag{17}$$

and $\delta(\cdot)$ denotes the first variation operator, T is the kinetic energy, H_e is the electric enthalpy and W_e is the work performed by the external forces. $[C]$ is the elastic coefficient matrix, $[e]$ is the piezoelectric coefficient matrix and $[\varepsilon]$ is the dielectric coefficient matrix. $\{u\}$ denotes the displacements field vector and $\{\dot{u}\}$ is the first time derivative of the displacements field vector. $\{\varepsilon\}$ is the strain vector, $\{E\}$ is the electric field vector and q is the distributed forces along the length of the beam. Substituting Equations (15)–(17) into Equation (14), integrating by parts and collecting the coefficients of δw , $\delta \varphi$ and $\delta \bar{\varphi}$, the governing equations and the associated boundary conditions in terms of elastic displacements and electric field variables are derived.

The equations of motion for the piezoelectric beam are as follows:

$$- A_0 \tilde{c}_{11} b \frac{\partial^4 w}{\partial x^4} + B_0 \tilde{c}_{11} b \frac{\partial^3 \varphi}{\partial x^3} + A_0 \rho b \frac{\partial^4 w}{\partial x^2 \partial t^2} - B_0 \rho b \frac{\partial^3 \varphi}{\partial x \partial t^2} - \rho b h \frac{\partial^2 w}{\partial t^2} + \tilde{e}_{31} b K_0 \frac{\partial^2 \bar{\varphi}}{\partial x^2} + q = 0, \tag{18}$$

$$- B_0 \tilde{c}_{11} b \frac{\partial^3 w}{\partial x^3} + C_0 \tilde{c}_{11} b \frac{\partial^2 \varphi}{\partial x^2} - D_0 c_{55} b \varphi - C_0 \rho b \frac{\partial^2 \varphi}{\partial t^2} + B_0 \rho b \frac{\partial^3 w}{\partial x \partial t^2} + \tilde{e}_{31} b L_0 \frac{\partial \bar{\varphi}}{\partial x} - e_{15} b N_0 \frac{\partial \bar{\varphi}}{\partial x} = 0, \tag{19}$$

$$\tilde{e}_{31} b K_0 \frac{\partial^2 w}{\partial x^2} + e_{15} b N_0 \frac{\partial \varphi}{\partial x} - \tilde{e}_{31} b L_0 \frac{\partial \varphi}{\partial x} - P_0 b \varepsilon_{11} \frac{\partial^2 \bar{\varphi}}{\partial x^2} + M_0 b \tilde{e}_{33} \bar{\varphi} = 0. \tag{20}$$

The boundary conditions at $x = 0$ and $x = L$ are as follows:

$$A_0 \tilde{c}_{11} b \frac{\partial^3 w}{\partial x^3} - B_0 \tilde{c}_{11} b \frac{\partial^2 \varphi}{\partial x^2} - A_0 \frac{\partial^3 w}{\partial x \partial t^2} + B_0 \frac{\partial^2 \varphi}{\partial t^2} - \tilde{e}_{31} b K_0 \frac{\partial \bar{\varphi}}{\partial x} = 0 \quad \text{or } w \text{ prescribed,} \tag{21}$$

$$- A_0 \tilde{c}_{11} b \frac{\partial^2 w}{\partial x^2} + B_0 \tilde{c}_{11} b \frac{\partial \varphi}{\partial x} + \tilde{e}_{31} b K_0 \bar{\varphi}(x, t) = 0 \quad \text{or } \frac{\partial w}{\partial x} \text{ prescribed,} \tag{22}$$

$$B_0 \tilde{c}_{11} b \frac{\partial^2 w}{\partial x^2} - C_0 \tilde{c}_{11} b \frac{\partial \varphi}{\partial x} - \tilde{e}_{31} b L_0 \bar{\varphi}(x, t) = 0 \quad \text{or } \varphi \text{ prescribed,} \tag{23}$$

$$P_0 b \varepsilon_{11} \frac{\partial \bar{\varphi}}{\partial x} - e_{15} b N_0 \varphi(x, t) = 0 \quad \text{or } \bar{\varphi} \text{ prescribed,} \tag{24}$$

where the coefficients A_0 , B_0 , C_0 , D_0 , K_0 , L_0 , M_0 , N_0 and P_0 are defined as follows:

$$\begin{aligned} A_0 &= \int_{z=-\frac{h}{2}}^{z=\frac{h}{2}} z^2 dz, & B_0 &= \int_{z=-\frac{h}{2}}^{z=\frac{h}{2}} z f(z) dz, & C_0 &= \int_{z=-\frac{h}{2}}^{z=\frac{h}{2}} [f(z)]^2 dz, \\ D_0 &= \int_{z=-\frac{h}{2}}^{z=\frac{h}{2}} [f'(z)]^2 dz, & K_0 &= \int_{z=-\frac{h}{2}}^{z=\frac{h}{2}} z g'(z) dz, & L_0 &= \int_{z=-\frac{h}{2}}^{z=\frac{h}{2}} f(z) g'(z) dz, \\ M_0 &= \int_{z=-\frac{h}{2}}^{z=\frac{h}{2}} [g'(z)]^2 dz, & N_0 &= \int_{z=-\frac{h}{2}}^{z=\frac{h}{2}} g(z) f'(z) dz, & P_0 &= \int_{z=-\frac{h}{2}}^{z=\frac{h}{2}} [g(z)]^2 dz. \end{aligned} \tag{25}$$

The coefficients A_0 , B_0 , C_0 and D_0 are related to the elastic properties and the coefficients K_0 , L_0 , M_0 , N_0 and P_0 are related to the piezoelectric properties of the beam.

4. Bending Analysis of the Piezoelectric Beam

The bending problem of a simply supported piezoelectric beam which is subjected to transverse load $q(x)$, as shown in Figure 2, is solved. For a beam simply supported and grounded at two ends, the end conditions are given by $\sigma_x = w = \bar{\varphi} = 0$ at $x = 0, L$ and $-h/2 \leq z \leq h/2$.

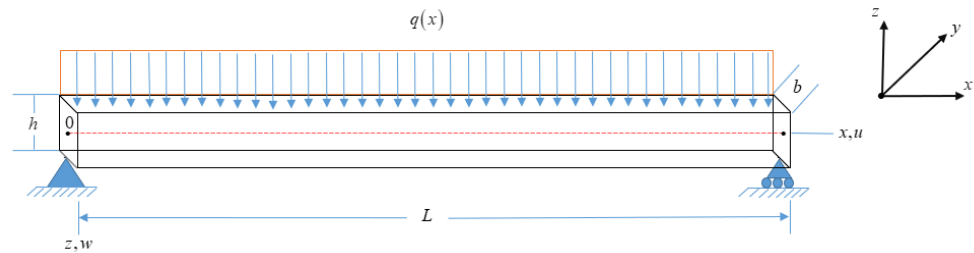


Figure 2. Geometry of a piezoelectric beam with simply supported boundary conditions, subjected to uniformly distributed load $q(x)$.

The governing equations for bending analysis of a piezoelectric beam (static case) are derived from Equations (18)–(20) discarding all terms containing time derivatives, as follows:

$$A_0 \tilde{c}_{11} b \frac{\partial^4 w}{\partial x^4} - B_0 \tilde{c}_{11} b \frac{\partial^3 \varphi}{\partial x^3} - K_0 \tilde{e}_{31} b \frac{\partial^2 \bar{\varphi}}{\partial x^2} = q, \tag{26}$$

$$B_0 \tilde{c}_{11} b \frac{\partial^3 w}{\partial x^3} - C_0 \tilde{c}_{11} b \frac{\partial^2 \varphi}{\partial x^2} + D_0 c_{55} b \varphi(x, t) - L_0 \tilde{e}_{31} b \frac{\partial \bar{\varphi}}{\partial x} + N_0 e_{15} b \frac{\partial \bar{\varphi}}{\partial x} = 0, \tag{27}$$

$$-K_0 \tilde{e}_{31} b \frac{\partial^2 w}{\partial x^2} + L_0 \tilde{e}_{31} b \frac{\partial \varphi}{\partial x} + P_0 b \in_{11} \frac{\partial^2 \bar{\varphi}}{\partial x^2} - N_0 e_{15} b \frac{\partial \varphi}{\partial x} - M_0 b \tilde{\epsilon}_{33} \bar{\varphi}(x, t) = 0. \tag{28}$$

The solution can be derived using the Fourier series method. The expansions are introduced in forms of sine and cosine series in order to satisfy the boundary conditions, as follows:

$$w(x) = \sum_{m=1}^{\infty} w_m \sin \frac{m\pi x}{L}, \tag{29}$$

$$\varphi(x) = \sum_{m=1}^{\infty} \varphi_m \cos \frac{m\pi x}{L}, \tag{30}$$

$$\bar{\varphi}(x) = \sum_{m=1}^{\infty} \bar{\varphi}_m \sin \frac{m\pi x}{L}, \tag{31}$$

$$q(x) = \sum_{m=1}^{\infty} q_m \sin \frac{m\pi x}{L}, \text{ with } q_m = \frac{4q_0}{m\pi} \text{ for } m = 1, 3, 5, \dots \tag{32}$$

and $q_m = 0$ for $m = 2, 4, 6, \dots$

The expansions (Equations (29)–(32)) are introduced in Equations (26)–(28), and an algebraic system with three variables results as follows:

$$\left(A_0 \tilde{c}_{11} b \frac{m^4 \pi^4}{L^4} \right) w_m - \left(B_0 \tilde{c}_{11} b \frac{m^3 \pi^3}{L^3} \right) \varphi_m + \left(\tilde{e}_{31} b K_0 \frac{m^2 \pi^2}{L^2} \right) \bar{\varphi}_m = q_m, \tag{33}$$

$$- \left(B_0 \tilde{c}_{11} b \left(\frac{m\pi}{L} \right)^3 \right) w_m + \left(C_0 \tilde{c}_{11} b \left(\frac{m\pi}{L} \right)^2 + D_0 c_{55} b \right) \varphi_m + (-L_0 \tilde{e}_{31} b + N_0 e_{15} b) \left(\frac{m\pi}{L} \right) \bar{\varphi}_m = 0, \tag{34}$$

$$K_0 \tilde{e}_{31} b \left(\frac{m\pi}{L} \right)^2 w_m + \left(-L_0 \tilde{e}_{31} b \left(\frac{m\pi}{L} \right) + N_0 e_{15} b \left(\frac{m\pi}{L} \right) \right) \varphi_m - \left(P_0 b \in_{11} \left(\frac{m\pi}{L} \right)^2 + M_0 b \tilde{\epsilon}_{33} \right) \bar{\varphi}_m = 0. \tag{35}$$

The above system is solved using the method of determinants, where the related determinants of the coefficients are as follows:

$$D = \det \begin{bmatrix} A_0\tilde{c}_{11}b\frac{m^4\pi^4}{L^4} & -B_0\tilde{c}_{11}b\frac{m^3\pi^3}{L^3} & K_0\tilde{e}_{31}b\frac{m^2\pi^2}{L^2} \\ -B_0\tilde{c}_{11}b\frac{m^3\pi^3}{L^3} & C_0\tilde{c}_{11}b\frac{m^2\pi^2}{L^2} + D_0c_{55}b & -L_0\tilde{e}_{31}b\frac{m\pi}{L} + N_0e_{15}b\frac{m\pi}{L} \\ K_0\tilde{e}_{31}b\frac{m^2\pi^2}{L^2} & -L_0\tilde{e}_{31}b\frac{m\pi}{L} + N_0e_{15}b\frac{m\pi}{L} & -P_0b \in_{11} \frac{m^2\pi^2}{L^2} - M_0b\tilde{\epsilon}_{33} \end{bmatrix}, \quad (36)$$

$$D_{w_m} = \det \begin{bmatrix} q_m & -B_0\tilde{c}_{11}b\frac{m^3\pi^3}{L^3} & K_0\tilde{e}_{31}b\frac{m^2\pi^2}{L^2} \\ 0 & C_0\tilde{c}_{11}b\frac{m^2\pi^2}{L^2} + D_0c_{55}b & -L_0\tilde{e}_{31}b\frac{m\pi}{L} + N_0e_{15}b\frac{m\pi}{L} \\ 0 & -L_0\tilde{e}_{31}b\frac{m\pi}{L} + N_0e_{15}b\frac{m\pi}{L} & -P_0b \in_{11} \frac{m^2\pi^2}{L^2} - M_0b\tilde{\epsilon}_{33} \end{bmatrix}, \quad (37)$$

$$D_{\varphi_m} = \det \begin{bmatrix} A_0\tilde{c}_{11}b\frac{m^4\pi^4}{L^4} & q_m & K_0\tilde{e}_{31}b\frac{m^2\pi^2}{L^2} \\ -B_0\tilde{c}_{11}b\frac{m^3\pi^3}{L^3} & 0 & -L_0\tilde{e}_{31}b\frac{m\pi}{L} + N_0e_{15}b\frac{m\pi}{L} \\ K_0\tilde{e}_{31}b\frac{m^2\pi^2}{L^2} & 0 & -P_0b \in_{11} \frac{m^2\pi^2}{L^2} - M_0b\tilde{\epsilon}_{33} \end{bmatrix}, \quad (38)$$

$$D_{\bar{\varphi}_m} = \det \begin{bmatrix} A_0\tilde{c}_{11}b\frac{m^4\pi^4}{L^4} & -B_0\tilde{c}_{11}b\frac{m^3\pi^3}{L^3} & q_m \\ -B_0\tilde{c}_{11}b\frac{m^3\pi^3}{L^3} & C_0\tilde{c}_{11}b\frac{m^2\pi^2}{L^2} + D_0c_{55}b & 0 \\ K_0\tilde{e}_{31}b\frac{m^2\pi^2}{L^2} & -L_0\tilde{e}_{31}b\frac{m\pi}{L} + N_0e_{15}b\frac{m\pi}{L} & 0 \end{bmatrix}. \quad (39)$$

Then, the general solution of the system has the following form:

$$w_m = \frac{q_m \left[(C_0\tilde{c}_{11}ba_m^2 + D_0c_{55}b)(-P_0b \in_{11} a_m^2 - M_0b\tilde{\epsilon}_{33}) - (-L_0\tilde{e}_{31}ba_m + N_0e_{15}ba_m)^2 \right]}{\left[(A_0\tilde{c}_{11}ba_m^4 (C_0\tilde{c}_{11}ba_m^2 + D_0c_{55}b) - (B_0\tilde{c}_{11}ba_m^3)^2 \right] (-P_0b \in_{11} a_m^2 - M_0b\tilde{\epsilon}_{33}) + (-B_0\tilde{c}_{11}ba_m^3 (-L_0\tilde{e}_{31}ba_m + N_0e_{15}ba_m) - (C_0\tilde{c}_{11}ba_m^2 + D_0c_{55}b) (K_0\tilde{e}_{31}ba_m^2)) (K_0\tilde{e}_{31}ba_m^2) + ((-B_0\tilde{c}_{11}ba_m^3) (K_0\tilde{e}_{31}ba_m^2) - A_0\tilde{c}_{11}ba_m^4 (-L_0\tilde{e}_{31}ba_m + N_0e_{15}ba_m)) (-L_0\tilde{e}_{31}ba_m + N_0e_{15}ba_m)} \quad (40)$$

$$\varphi_m = \frac{-q_m \left[-B_0\tilde{c}_{11}ba_m^3 (-P_0b \in_{11} a_m^2 - M_0b\tilde{\epsilon}_{33}) - (-L_0\tilde{e}_{31}ba_m + N_0e_{15}ba_m) (K_0\tilde{e}_{31}ba_m^2) \right]}{\left[(A_0\tilde{c}_{11}ba_m^4 (C_0\tilde{c}_{11}ba_m^2 + D_0c_{55}b) - (B_0\tilde{c}_{11}ba_m^3)^2 \right] (-P_0b \in_{11} a_m^2 - M_0b\tilde{\epsilon}_{33}) + (-B_0\tilde{c}_{11}ba_m^3 (-L_0\tilde{e}_{31}ba_m + N_0e_{15}ba_m) - (C_0\tilde{c}_{11}ba_m^2 + D_0c_{55}b) (K_0\tilde{e}_{31}ba_m^2)) (K_0\tilde{e}_{31}ba_m^2) + ((-B_0\tilde{c}_{11}ba_m^3) (K_0\tilde{e}_{31}ba_m^2) - A_0\tilde{c}_{11}ba_m^4 (-L_0\tilde{e}_{31}ba_m + N_0e_{15}ba_m)) (-L_0\tilde{e}_{31}ba_m + N_0e_{15}ba_m)} \quad (41)$$

$$\bar{\varphi}_m = \frac{q_m \left[-B_0\tilde{c}_{11}ba_m^3 (-L_0\tilde{e}_{31}ba_m + N_0e_{15}ba_m) - (C_0\tilde{c}_{11}ba_m^2 + D_0c_{55}b) (K_0\tilde{e}_{31}ba_m^2) \right]}{\left[(A_0\tilde{c}_{11}ba_m^4 (C_0\tilde{c}_{11}ba_m^2 + D_0c_{55}b) - (B_0\tilde{c}_{11}ba_m^3)^2 \right] (-P_0b \in_{11} a_m^2 - M_0b\tilde{\epsilon}_{33}) + (-B_0\tilde{c}_{11}ba_m^3 (-L_0\tilde{e}_{31}ba_m + N_0e_{15}ba_m) - (C_0\tilde{c}_{11}ba_m^2 + D_0c_{55}b) (K_0\tilde{e}_{31}ba_m^2)) (K_0\tilde{e}_{31}ba_m^2) + ((-B_0\tilde{c}_{11}ba_m^3) (K_0\tilde{e}_{31}ba_m^2) - A_0\tilde{c}_{11}ba_m^4 (-L_0\tilde{e}_{31}ba_m + N_0e_{15}ba_m)) (-L_0\tilde{e}_{31}ba_m + N_0e_{15}ba_m)} \quad (42)$$

Using the above values of the coefficients w_m , φ_m and $\bar{\varphi}_m$ in Equations (29)–(31), the final expressions of w , φ and $\bar{\varphi}$ are obtained. Then, using the final expressions of w , φ and $\bar{\varphi}$, in Equations (1), (3), (4), (7)–(10), final expressions for axial displacement u , transverse displacement w , electric potential $\bar{\varphi}$, axial bending stress σ_x , transverse shear stress τ_{xz} , axial electric displacement D_x and transverse electric displacement D_z are obtained, as follows:

Axial displacement:

$$u = \sum_{m=1}^{\infty} \left\{ \left[-z \frac{m\pi}{L} w_m + f(z) \varphi_m \right] \cos \frac{m\pi x}{L} \right\}. \quad (43)$$

Transverse displacement:

$$w = \sum_{m=1}^{\infty} \left\{ [w_m] \sin \frac{m\pi x}{L} \right\}. \quad (44)$$

Electric potential:

$$\tilde{\varphi} = \sum_{m=1}^{\infty} \left\{ [g(z)\bar{\varphi}_m] \sin \frac{m\pi x}{L} \right\}. \tag{45}$$

Axial bending stress:

$$\sigma_x = \sum_{m=1}^{\infty} \left\{ \left[\tilde{c}_{11} z \frac{m^2 \pi^2}{L^2} w_m - \tilde{c}_{11} f(z) \frac{m\pi}{L} \varphi_m + \tilde{e}_{31} g'(z) \bar{\varphi}_m \right] \sin \frac{m\pi x}{L} \right\}. \tag{46}$$

Transverse shear stress:

$$\tau_{xz} = \sum_{m=1}^{\infty} \left\{ \left[c_{55} f'(z) \varphi_m + e_{15} g(z) \frac{m\pi}{L} \bar{\varphi}_m \right] \cos \frac{m\pi x}{L} \right\}. \tag{47}$$

Axial electric displacement:

$$D_x = \sum_{m=1}^{\infty} \left\{ \left[e_{15} f'(z) \varphi_m - \epsilon_{11} g(z) \frac{m\pi}{L} \bar{\varphi}_m \right] \cos \frac{m\pi x}{L} \right\}. \tag{48}$$

Transverse electric displacement:

$$D_z = \sum_{m=1}^{\infty} \left\{ \left[\tilde{e}_{31} z \frac{m^2 \pi^2}{L^2} w_m - \tilde{e}_{31} f(z) \frac{m\pi}{L} \varphi_m - \tilde{\epsilon}_{33} g'(z) \bar{\varphi}_m \right] \sin \frac{m\pi x}{L} \right\}. \tag{49}$$

5. Free Flexural Vibration Analysis of the Piezoelectric Beam

The governing equations for the free flexural vibration problem of a simply supported piezoelectric beam can be obtained by setting the applied transverse load $q(x)$ equal to zero in Equations (18)–(20). A solution of the resulting governing equations, which satisfies the associated initial conditions, is of the following form:

$$w(x, t) = \sum_{m=1}^{\infty} w_m \sin \left(\frac{m\pi x}{L} \right) \sin(\omega_m t), \tag{50}$$

$$\varphi(x, t) = \sum_{m=1}^{\infty} \varphi_m \cos \left(\frac{m\pi x}{L} \right) \sin(\omega_m t), \tag{51}$$

$$\bar{\varphi}(x, t) = \sum_{m=1}^{\infty} \bar{\varphi}_m \sin \left(\frac{m\pi x}{L} \right) \sin(\omega_m t), \tag{52}$$

where w_m , φ_m and $\bar{\varphi}_m$ are the amplitudes of transverse displacement, rotation and electric potential, respectively, and ω_m is the natural frequency of the m^{th} mode of vibration. Substitution of these solution forms into the governing equations of free vibration of piezoelectric beam results in the following linear algebraic equation system:

$$\left[(A_0 \tilde{c}_{11} b \alpha_m^4) w_m - (B_0 \tilde{c}_{11} b \alpha_m^3) \varphi_m + (K_0 \tilde{e}_{31} b \alpha_m^2) \bar{\varphi}_m \right] - \omega_m^2 \left[(A_0 \rho b \alpha_m^2 + \rho b h) w_m - (B_0 \rho b a_m) \varphi_m \right] = 0, \tag{53}$$

$$\left[(-B_0 \tilde{c}_{11} b \alpha_m^3) w_m + (C_0 \tilde{c}_{11} b \alpha_m^2 + D_0 c_{55} b) \varphi_m + (-L_0 \tilde{e}_{31} b a_m + N_0 e_{15} b a_m) \bar{\varphi}_m \right] - \omega_m^2 \left[(-B_0 \rho b a_m) w_m + (C_0 \rho b) \varphi_m \right] = 0, \tag{54}$$

$$\left[(K_0 \tilde{e}_{31} b a_m^2) w_m + (-L_0 \tilde{e}_{31} b a_m + N_0 e_{15} b a_m) \varphi_m - (P_0 \epsilon_{11} b a_m^2 + M_0 \tilde{\epsilon}_{33} b) \bar{\varphi}_m \right] = 0. \tag{55}$$

The Equations (53)–(55) can be written in the following matrix form:

$$\left(\begin{bmatrix} K_{11} & K_{12} & K_{13} \\ K_{21} & K_{22} & K_{23} \\ K_{31} & K_{32} & K_{33} \end{bmatrix} - \omega_m^2 \begin{bmatrix} M_{11} & M_{12} & 0 \\ M_{21} & M_{22} & 0 \\ 0 & 0 & 0 \end{bmatrix} \right) \begin{Bmatrix} w_m \\ \varphi_m \\ \bar{\varphi}_m \end{Bmatrix} = 0. \tag{56}$$

Equation (56) can be written in the following, more compact form:

$$([K] - \omega_m^2[M])\{\Delta\} = 0 \tag{57}$$

where $\{\Delta\}^T = \{\omega_m, \varphi_m, \tilde{\varphi}_m\}$. The $[K]$ and $[M]$ are symmetric matrices, so we have $K_{12} = K_{21}$, $K_{13} = K_{31}$, $K_{23} = K_{32}$ and $M_{12} = M_{21}$.

The elements of the coefficient matrix $[K]$ are given by the following:

$$\begin{aligned} K_{11} &= A_0\tilde{c}_{11}b\alpha_m^4, \\ K_{12} = K_{21} &= -B_0\tilde{c}_{11}b\alpha_m^3, \\ K_{13} = K_{31} &= K_0\tilde{e}_{31}ba_m^2, \\ K_{22} &= C_0\tilde{c}_{11}b\alpha_m^2 + D_0c_{55}b, \\ K_{23} = K_{32} &= -L_0\tilde{e}_{31}ba_m + N_0e_{15}ba_m, \\ K_{33} &= -P_0\epsilon_{11}ba_m^2 - M_0\tilde{\epsilon}_{33}b. \end{aligned} \tag{58}$$

The elements of the coefficient matrix $[M]$ are given by the following:

$$\begin{aligned} M_{11} &= A_0\rho b\alpha_m^2 + \rho bh, \\ M_{12} = M_{21} &= -B_0\rho ba_m, \\ M_{22} &= C_0\rho b. \end{aligned} \tag{59}$$

For nontrivial solutions of Equation (57), the necessary condition is expressed as follows:

$$\det([K] - \omega_m^2[M]) = 0. \tag{60}$$

The solution of the above equation yields the values of the eigen-frequencies ω_m for various modes of vibration of the piezoelectric beam. Expanding Equation (60) gives the following:

$$\det \left(\begin{bmatrix} K_{11} & K_{12} & K_{13} \\ K_{21} & K_{22} & K_{23} \\ K_{31} & K_{32} & K_{33} \end{bmatrix} - \begin{bmatrix} \omega_m^2 M_{11} & \omega_m^2 M_{12} & 0 \\ \omega_m^2 M_{21} & \omega_m^2 M_{22} & 0 \\ 0 & 0 & 0 \end{bmatrix} \right) = 0. \tag{61}$$

After the necessary calculations, the following fourth order algebraic equation is obtained:

$$\begin{aligned} &\omega_m^4(K_{33}M_{11}M_{22} - K_{33}M_{12}M_{12}) + \\ &+ \omega_m^2 \left(-K_{11}K_{33}M_{22} - K_{22}K_{33}M_{11} + K_{23}K_{23}M_{11} + K_{12}K_{33}M_{12} + \right. \\ &\quad \left. + K_{12}K_{33}M_{12} - K_{13}K_{23}M_{12} - K_{13}K_{23}M_{12} + K_{13}K_{13}M_{22} \right) + \\ &+ (K_{11}K_{22}K_{33} - K_{11}K_{23}K_{23} - K_{12}K_{12}K_{33} + K_{12}K_{13}K_{23} + K_{12}K_{13}K_{23} - K_{13}K_{13}K_{22}) = 0. \end{aligned} \tag{62}$$

From the solution of the above equation, four roots are obtained: two positive frequencies ω_w, ω_φ and two negative conjugate frequencies which are rejected. The first frequency ω_w is the flexural frequency and the second ω_φ is the fundamental frequency of thickness shear mode of the piezoelectric beam. The results for the fundamental frequency ω_m are presented in the following non-dimensional form:

$$\bar{\omega} = \omega_m \left(\frac{L^2}{h} \right) \sqrt{\frac{\rho}{\tilde{c}_{11}}}. \tag{63}$$

6. Numerical Results and Discussion

For the examples and numerical calculations, a simply supported piezoelectric beam is considered, as shown in Figure 2, with length $L = 0.6$ m, thickness $b = 0.002$ m and height h . The value of the height h depends on the aspect ratio ($S = L/h$) values. Zero electric potential $\tilde{\varphi}$ at the upper and lower ($x, z = \pm h/2$) surface of the beam is considered (short circuit electric conditions) and for this reason, a TYPE II expression of the function $g(z) = 1 - (\frac{2z}{h})^2$ is chosen. In the static problem, the beam is subjected to a uniformly

distributed exterior load $q_0 = 10 \text{ N/m}^2$ ($q^* = q_0/b$ for the results presented below). The piezoelectric material of the beam is PZT-4 [28], with density $\rho = 7500 \text{ kg/m}^3$ and an elastic coefficient matrix as follows:

$$[C] = \begin{bmatrix} c_{11} & c_{12} & c_{13} & 0 & 0 & 0 \\ c_{21} & c_{22} & c_{23} & 0 & 0 & 0 \\ c_{31} & c_{32} & c_{33} & 0 & 0 & 0 \\ 0 & 0 & 0 & c_{44} & 0 & 0 \\ 0 & 0 & 0 & 0 & c_{55} & 0 \\ 0 & 0 & 0 & 0 & 0 & c_{66} \end{bmatrix} = \begin{bmatrix} 139 & 77.8 & 74.3 & 0 & 0 & 0 \\ 77.8 & 139 & 74.3 & 0 & 0 & 0 \\ 74.3 & 74.3 & 11.3 & 0 & 0 & 0 \\ 0 & 0 & 0 & 25.6 & 0 & 0 \\ 0 & 0 & 0 & 0 & 25.6 & 0 \\ 0 & 0 & 0 & 0 & 0 & 30.6 \end{bmatrix} \text{ GPa.} \quad (64)$$

It has a piezoelectric coefficient matrix as follows:

$$[e] = \begin{bmatrix} 0 & 0 & 0 & 0 & e_{15} & 0 \\ 0 & 0 & 0 & e_{15} & 0 & 0 \\ e_{31} & e_{32} & e_{33} & 0 & 0 & 0 \end{bmatrix} = \begin{bmatrix} 0 & 0 & 0 & 0 & 13.44 & 0 \\ 0 & 0 & 0 & 13.44 & 0 & 0 \\ -6.98 & -6.98 & 13.84 & 0 & 0 & 0 \end{bmatrix} \frac{\text{C}}{\text{m}^2}. \quad (65)$$

Moreover, it has a dielectric coefficient matrix as follows:

$$[\epsilon] = \begin{bmatrix} \epsilon_{11} & 0 & 0 \\ 0 & \epsilon_{22} & 0 \\ 0 & 0 & \epsilon_{33} \end{bmatrix} = \begin{bmatrix} 6.00 & 0 & 0 \\ 0 & 6.00 & 0 \\ 0 & 0 & 5.47 \end{bmatrix} \times 10^{-9} \frac{\text{V}}{\text{C} \cdot \text{m}}. \quad (66)$$

6.1. Bending Analysis of the Piezoelectric Beam

For the bending analysis of the piezoelectric beam, the transverse displacement w , the rotation φ and the electric potential $\tilde{\varphi}$ are calculated for all models of the beam with various aspect ratios ($S = 2, 5, 10, 30$), and the obtained results are presented in Table 3.

Table 3. Comparison of transverse displacement w at the center of the beam ($x = L/2$), rotation φ at the end of the beam ($x = 0$) and electric potential $\tilde{\varphi}$ at the center of the beam ($x = L/2, z = 0$) for linear high order shear deformation theories of piezoelectric beams with aspect ratios $S = 2, 5, 10, 30$.

Aspect Ratio S	Model	Transverse Displacement $w(m)$	Rotation $\varphi(^{\circ})$	Electric Potential $\tilde{\varphi}(V)$
2	Ambartsumian [12]	$-1.2801112 \times 10^{-10}$	2.0286439×10^{-8}	-0.039315504
	Kruszewski [13]	$-1.2803252 \times 10^{-10}$	5.1231438×10^{-8}	-0.039319084
	Reddy [14]	$-1.2803614 \times 10^{-10}$	2.2822244×10^{-8}	-0.039315504
	Touratier [15]	$-1.2794482 \times 10^{-10}$	2.3494154×10^{-8}	-0.039296693
	Karama [18]	$-1.2752185 \times 10^{-10}$	2.4067348×10^{-8}	-0.039176182
	Soldatos [17]	$-1.2800025 \times 10^{-10}$	2.1782638×10^{-8}	-0.040582753
	Exact Solution [28]	$-1.2955144 \times 10^{-10}$	–	–
5	Ambartsumian [12]	$-1.3902144 \times 10^{-9}$	3.5580401×10^{-8}	-0.071643269
	Kruszewski [13]	$-1.3906821 \times 10^{-9}$	3.1694925×10^{-8}	-0.071660602
	Reddy [14]	$-1.3903140 \times 10^{-9}$	6.4044722×10^{-8}	-0.071643269
	Touratier [15]	$-1.3905663 \times 10^{-9}$	6.6076112×10^{-8}	-0.071656142
	Karama [18]	$-1.3896790 \times 10^{-9}$	6.7971740×10^{-8}	-0.071614474
	Soldatos [17]	$-1.3902219 \times 10^{-9}$	5.0052762×10^{-8}	-0.072021637
	Exact Solution [28]	$-1.3854365 \times 10^{-9}$	–	–
10	Ambartsumian [12]	$-1.0365670 \times 10^{-8}$	1.2937340×10^{-7}	-0.134659590
	Kruszewski [13]	$-1.0369451 \times 10^{-8}$	1.0574177×10^{-7}	-0.134695396
	Reddy [14]	$-1.0366002 \times 10^{-8}$	1.3218032×10^{-7}	-0.134659590
	Touratier [15]	$-1.0369253 \times 10^{-8}$	1.3643415×10^{-7}	-0.134693113
	Karama [18]	$-1.0367532 \times 10^{-8}$	1.4046581×10^{-7}	-0.134672500
	Soldatos [17]	$-1.0365697 \times 10^{-8}$	1.0331467×10^{-7}	-0.134839081
	Exact Solution [28]	$-1.0353429 \times 10^{-8}$	–	–

Table 3. Cont.

Aspect Ratio S	Model	Transverse Displacement $w(m)$	Rotation $\varphi(^{\circ})$	Electric Potential $\tilde{\varphi}(V)$
30	Ambartsumian [12]	$-2.7373816 \times 10^{-7}$	3.4080394×10^{-7}	-0.396536889
	Kruszewski [13]	$-2.7384038 \times 10^{-7}$	3.2157700×10^{-7}	-0.396645338
	Reddy [14]	$-2.7374235 \times 10^{-7}$	4.0197111×10^{-7}	-0.396536889
	Touratier [15]	$-2.7383981 \times 10^{-7}$	4.1498035×10^{-7}	-0.396644474
	Karama [18]	$-2.7383470 \times 10^{-7}$	4.2737985×10^{-7}	-0.396637526
	Soldatos [17]	$-2.7373825 \times 10^{-7}$	3.1420304×10^{-7}	-0.396597288
	Exact Solution [28]	$-2.7370209 \times 10^{-7}$	-	-0.397

Comparison of transverse displacement w and electric potential $\tilde{\varphi}$ for all models with higher order shear deformation terms through the length of the beam for various aspect ratios ($S = 2, 5, 10, 30$) are presented in Figures 3 and 4, respectively.

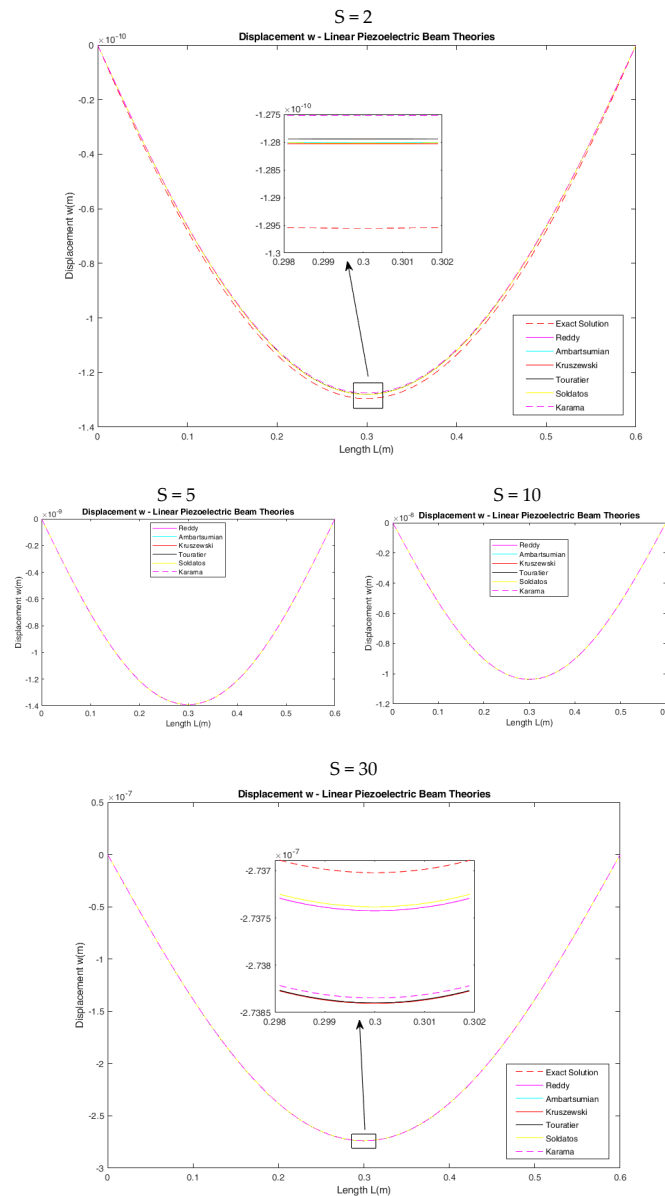


Figure 3. Comparison of transverse displacement w through the length of the beam at $(x, z = 0)$ for various aspect ratios ($S = 2, 5, 10, 30$) and for all models with higher order shear deformation terms.

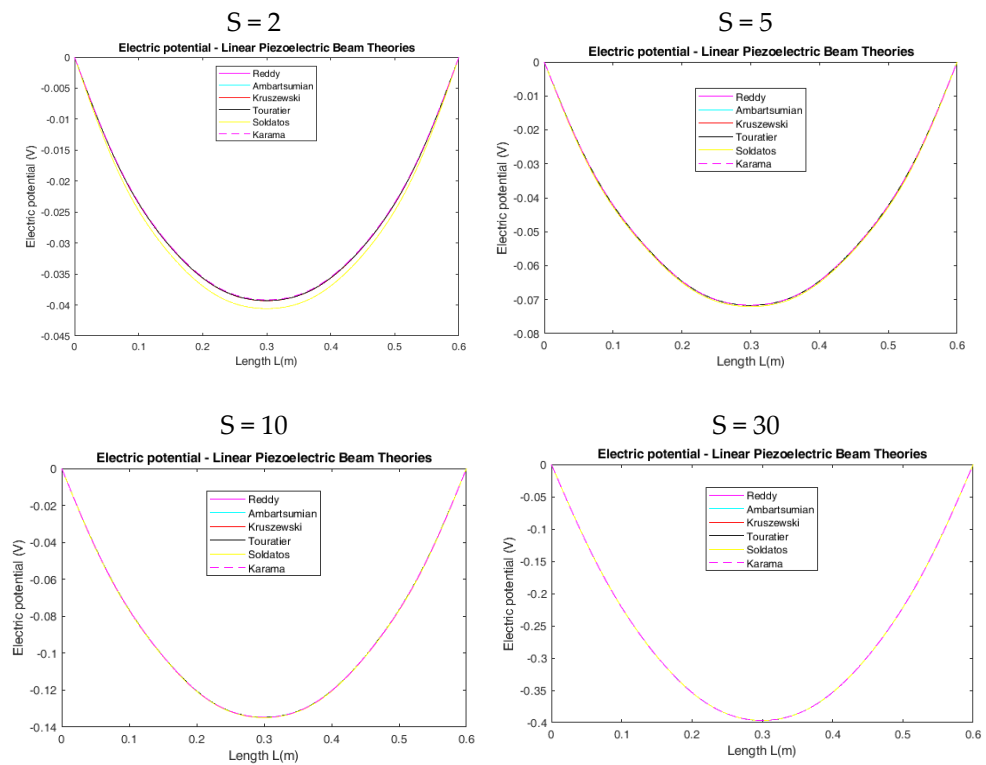


Figure 4. Comparison of electric potential $\tilde{\varphi}$ through the length of the beam at $(x, z = 0)$ for various aspect ratios ($S = 2, 5, 10, 30$) and for all models with higher order shear deformation terms.

From the above numerical results, it is concluded that the general model underestimates the maximum transverse displacement w for very thick beams ($S = 2$), while it overestimates w for thick ($S = 5, S = 10$) and slender ($S = 30$) beams. The maximum electric potential $\tilde{\varphi}$ predicted by the general model is in very good agreement with the exact solution for slender beams ($S = 30$).

Comparison of axial stress σ_x through the length of the beam at $(x, z = h/2)$ and through the height of the beam at $(x = L/2, z)$ for piezoelectric beams with aspect ratio $S = 30$ and for all models with higher order shear deformation terms are presented in Figures 5 and 6, respectively. In addition, comparison of transverse shear stress τ_{xz} through the length of the beam at $(x, z = h/4)$ and through the height of the beam at $(x = L/4, z)$ for all models with aspect ratio $S = 30$ are presented in Figures 7 and 8, respectively.

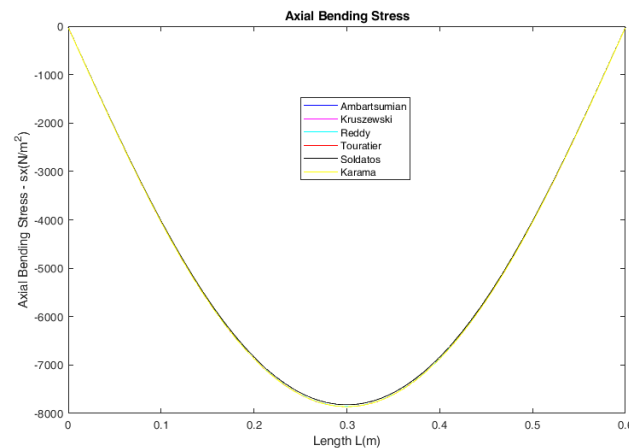


Figure 5. Comparison of axial stress σ_x through the length of the beam at $(x, z = h/2)$ for all models with aspect ratio $S = 30$.

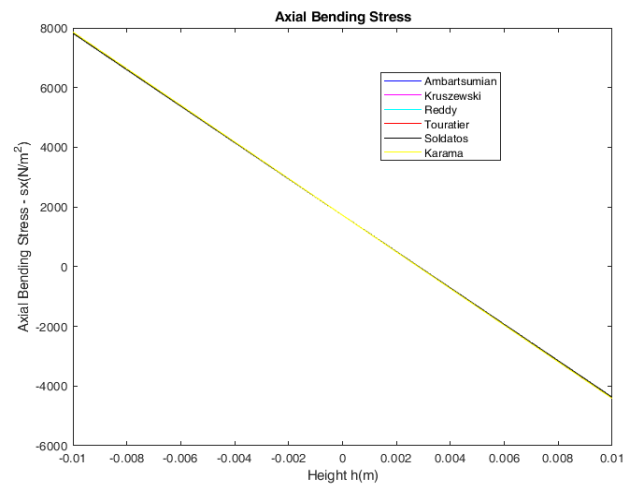


Figure 6. Comparison of axial stress σ_x through the height of the beam at $(x = L/2, z)$ for all models with aspect ratio $S = 30$.

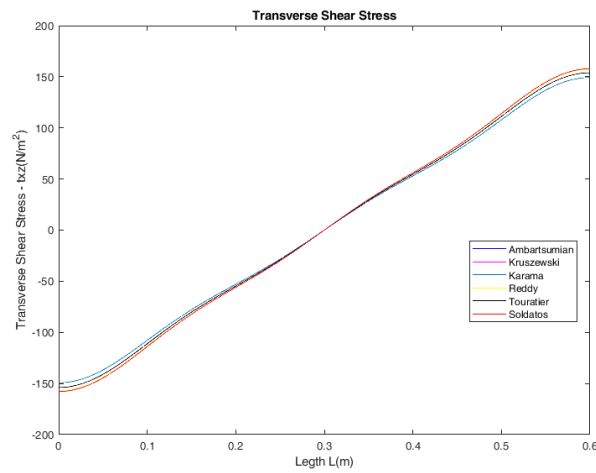


Figure 7. Comparison of transverse shear stress τ_{xz} through the length of the beam at $(x, z = h/4)$ for all models with aspect ratio $S = 30$.

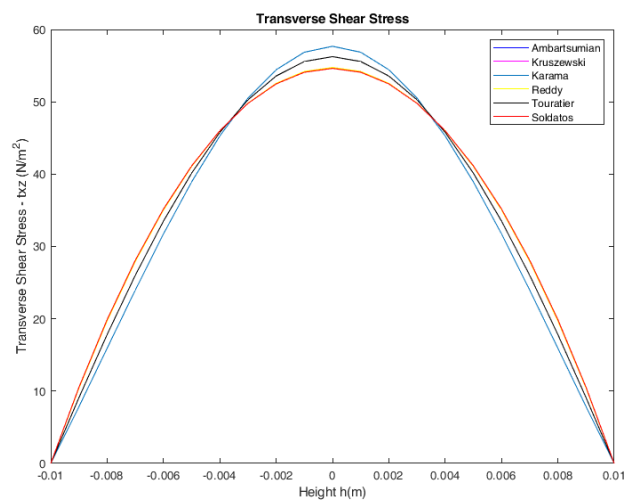


Figure 8. Comparison of transverse shear stress τ_{xz} through the height of the beam at $(x = L/4, z)$ for all models with aspect ratio $S = 30$.

From the numerical results presented in Table 4, it follows that the axial bending stress σ_x predicted by all models is in very good agreement with the exact solution for beams with aspect ratio $S = 30$. The maximum transverse shear stress τ_{xz} predicted by the Touratier model is in very good agreement with that from the exact solution. The models of Ambartsumian, Reddy and Soldatos underestimate while the model of Karama overestimates the value of transverse shear stress for beams with aspect ratio $S = 30$.

Table 4. Axial stress σ_x at $(x = L/2, z = -h/2)$ and transverse shear stress τ_{xz} at $(x = L/4, z = 0)$ for high order shear deformation models of piezoelectric beams with aspect ratio $S = 30$.

Models	Ambartsumian [12]	Kruszewski [13]	Reddy [14]	Touratier [15]	Karama [18]	Soldatos [17]	Exact Solution [28]
$\sigma_x \left(\frac{N}{m^2} \right)$	-7858.228	-7860.983	-7858.228	-7860.700	-7860.203	-7858.250	-7860
$\tau_{xz} \left(\frac{N}{m^2} \right)$	54.7450	54.7477	54.7450	56.2460	57.6778	54.6084	56

6.2. Free Flexural Vibration Analysis of the Piezoelectric Beam

For the free flexural vibration analysis of the piezoelectric beam, the non-dimensional flexural frequency $\bar{\omega}_w$ and the non-dimensional frequency of thickness shear mode $\bar{\omega}_\phi$ is calculated for various modes of vibration and various aspect ratios. The results are presented in Tables 5–7.

Table 5. Comparison of non-dimensional fundamental ($m = 1$) flexural and thickness shear mode frequencies of the piezoelectric beam.

Model	S=2		S=5		S=10		S=30	
	$\bar{\omega}_w$	$\bar{\omega}_\phi$	$\bar{\omega}_w$	$\bar{\omega}_\phi$	$\bar{\omega}_w$	$\bar{\omega}_\phi$	$\bar{\omega}_w$	$\bar{\omega}_\phi$
Ambartsumian [12]	2.3315	9.8072	2.8681	47.5546	3.0006	180.3669	3.0454	1595.544
Kruszewski [13]	2.3315	9.8072	2.8681	47.5546	3.0006	180.3669	3.0454	1595.544
Reddy [14]	2.3315	9.8072	2.8681	47.5546	3.0006	180.3669	3.0454	1595.544
Touratier [15]	2.3325	9.8022	2.8683	47.5255	3.0007	180.2522	3.0454	1594.517
Karama [18]	2.3358	9.8048	2.8692	47.5546	3.0010	180.3821	3.0454	1595.728
Soldatos [17]	2.3314	9.8080	2.8681	47.5599	3.0007	180.3882	3.0454	1595.736

Table 6. Comparison of non-dimensional flexural frequency $\bar{\omega}_w$ of the piezoelectric beam for various modes of vibration.

Aspect Ratio S	Model	Modes of Vibration				
		m=1	m=2	m=3	m=4	m=5
2	Ambartsumian [12]	2.3315	6.7289	11.7170	16.9055	22.1801
	Kruszewski [13]	2.3315	6.7289	11.7170	16.9055	22.1801
	Reddy [14]	2.3315	6.7289	11.7170	16.9055	22.1801
	Touratier [15]	2.3325	6.7382	11.7464	16.9693	22.2945
	Karama [18]	2.3358	6.7614	11.8122	17.1035	22.5246
	Soldatos [17]	2.3314	6.7280	11.7141	16.8994	22.1693
5	Ambartsumian [12]	2.8681	10.0322	19.5357	30.3754	42.0556
	Kruszewski [13]	2.8681	10.0322	19.5357	30.3754	42.0556
	Reddy [14]	2.8681	10.0322	19.5357	30.3754	42.0556
	Touratier [15]	2.8683	10.0350	19.5474	30.4050	42.1138
	Karama [18]	2.8692	10.0451	19.5826	30.4846	42.2589
	Soldatos [17]	2.8681	10.0319	19.5346	30.3726	42.0500

Table 6. Cont.

Aspect Ratio S	Model	Modes of Vibration				
		m=1	m=2	m=3	m=4	m=5
10	Ambartsumian [12]	3.0006	11.4726	24.2367	40.1288	58.2890
	Kruszewski [13]	3.0006	11.4726	24.2367	40.1288	58.2890
	Reddy [14]	3.0006	11.4726	24.2367	40.1288	58.2890
	Touratier [15]	3.0007	11.4735	24.2407	40.1403	58.3144
	Karama [18]	3.0010	11.4771	24.2561	40.1806	58.3957
	Soldatos [17]	3.0006	11.4726	24.2364	40.1279	58.2869
30	Ambartsumian [12]	3.0454	12.1132	27.0062	47.4207	72.9772
	Kruszewski [13]	3.0454	12.1132	27.0062	47.4207	72.9772
	Reddy [14]	3.0454	12.1132	27.0062	47.4207	72.9772
	Touratier [15]	3.0454	12.1133	27.0067	47.4222	72.9810
	Karama [18]	3.0454	12.1138	27.0090	47.4293	72.9974
	Soldatos [17]	3.0454	12.1132	27.0062	47.4206	72.9771

Table 7. Comparison of non-dimensional frequency of thickness shear mode $\bar{\omega}_\varphi$ of the piezoelectric beam for various modes of vibration.

Aspect Ratio S	Model	Modes of Vibration				
		m=1	m=2	m=3	m=4	m=5
2	Ambartsumian [12]	9.8072	14.9405	20.6814	26.6380	32.6955
	Kruszewski [13]	9.8072	14.9405	20.6814	26.6380	32.6955
	Reddy [14]	9.8072	14.9405	20.6814	26.6380	32.6955
	Touratier [15]	9.8022	14.9352	20.6761	26.6328	32.6905
	Karama [18]	9.8048	14.9352	20.6746	26.6305	32.6877
	Soldatos [17]	9.8080	14.9411	20.6819	26.6385	32.6959
5	Ambartsumian [12]	47.5546	55.9525	67.1314	79.8167	93.3781
	Kruszewski [13]	47.5546	55.9525	67.1314	79.8167	93.3781
	Reddy [14]	47.5546	55.9525	67.1314	79.8167	93.3781
	Touratier [15]	47.5255	55.9222	67.1000	79.7845	93.3454
	Karama [18]	47.5546	55.9423	67.1118	79.7896	93.3452
	Soldatos [17]	47.5599	55.9575	67.1361	79.8210	93.3820
10	Ambartsumian [12]	180.3669	190.2187	205.1441	223.8103	245.1810
	Kruszewski [13]	180.3669	190.2187	205.1441	223.8103	245.1810
	Reddy [14]	180.3669	190.2187	205.1441	223.8103	245.1810
	Touratier [15]	180.2522	190.1022	205.0251	223.6889	245.0572
	Karama [18]	180.3821	190.2186	205.1239	223.7694	245.1204
	Soldatos [17]	180.3882	190.2396	205.1645	223.8301	245.2002
30	Ambartsumian [12]	1595.5449	1606.0432	1623.3029	1646.9948	1676.7049
	Kruszewski [13]	1595.5449	1606.0432	1623.3029	1646.9948	1676.7049
	Reddy [14]	1595.5449	1606.0432	1623.3029	1646.9948	1676.7049
	Touratier [15]	1594.5170	1605.0133	1622.2698	1645.9573	1675.6621
	Karama [18]	1595.7288	1606.2091	1623.4397	1647.0929	1676.7564
	Soldatos [17]	1595.7368	1606.2347	1623.4939	1647.1849	1676.8941

From the above results, it follows that the values of flexural frequencies ω_w and thickness shear mode frequencies ω_φ are in excellent agreement with each other for all modes of vibration.

7. Potential Applications and Future Work

The unified shear deformation theory can contribute to a more accurate design of composite piezoelectric sensors and actuators for various mechanical applications.

The work will be extended at first to the bending and vibration problems of composite piezoelectric beams and plates with different important boundary conditions (clamped–clamped and clamped–free) and thermal effects will also be included.

Another extension of substantial interest will involve nonlocal strain gradient theory for the study of functionally gradient materials in micro- and nanoscale structures with size effects [32,33].

8. Conclusions

In this work, six models of elastic beam with high order shear deformation terms were extended for piezoelectric materials and grouped. The unified theory for shear deformation and electric potential distribution was used for the analysis of the static bending problem and the free flexural vibration problem of a piezoelectric beam with simply supported boundary conditions. From the study and comparison of the related numerical results, the following conclusions are drawn:

1. The transverse displacement w is maximum at the middle points of the beam ($x = L/2, z$) and the electric potential $\tilde{\varphi}$ is maximum in the middle plane of the beam ($x, z = 0$), for all models and aspect ratios S .
2. The general model underestimates the maximum transverse displacement w for very thick beams ($S = 2$) and overestimates the w for thick ($S = 5, S = 10$) and slender ($S = 30$) beams. The maximum electric potential $\tilde{\varphi}$ predicted by the general model is in very good agreement with the exact solution for slender beams ($S = 30$).
3. The maximum transverse shear stress τ_{xz} predicted by the Touratier model is in very good agreement with the corresponding result from the exact solution. The models of Ambartsumian, Reddy and Soldatos underestimate while the model of Karama overestimates the value of transverse shear stress for all aspect ratios.
4. The results of flexural frequencies ω_w and thickness shear mode frequencies ω_φ are in excellent agreement with each other for all modes of vibration.

Author Contributions: Conceptualization and methodology, K.I.N. and E.P.H.; investigation and analysis, K.I.N., K.G.B. and E.P.H.; software and writing—original draft preparation, K.I.N. and E.P.H.; supervision, writing—review and editing, K.G.B. and E.P.H. All authors have read and agreed to the published version of the manuscript.

Funding: The implementation of this research is co-financed by Greece and the European Union (European Social Fund-ESF) through the Operational Programme «Human Resources Development, Education and Lifelong Learning» in the context of the Act “Enhancing Human Resources Research Potential by undertaking Doctoral Research” Sub-action 2: IKY Scholarship Programme for PhD candidates in Greek Universities (MIS-5113934).



Data Availability Statement: Data are available from the corresponding authors upon reasonable request.

Conflicts of Interest: The authors declare no conflict of interest. The funders had no role in the design of the study; in the collection, analyses or interpretation of the data; in the writing of the manuscript; or in the decision to publish the results.

References

1. Ballas, R.G. *Piezoelectric Multilayer Beam Bending Actuators*, 1st ed.; Springer: Berlin/Heidelberg, Germany, 2007; pp. 47–75.
2. Gopinathan, S.V.; Varadan, V.V.; Varadan, V.K. A review and critique of theories for piezoelectric laminates. *Smart Mater. Struct.* **2000**, *9*, 24–48. [[CrossRef](#)]
3. Vlazov, V.Z.; Leontiev, U.N. *Beams, Plates and Shells on Elastic Foundation*; Israel Program for Scientific Translation Ltd.: Jerusalem, Israel, 1966.
4. Timoshenko, S.P. On the correction for shear of the differential equation for transverse vibrations of prismatic bars. *Philos. Mag.* **1921**, *41*, 742–746. [[CrossRef](#)]
5. Baluch, M.H.; Azad, A.K.; Khidir, M.A. Technical theory of beams with normal strain. *J. Eng. Mech. Proc. ASCE* **1984**, *110*, 1233–1237. [[CrossRef](#)]

6. Bhimaraddi, A.; Chandrashekhara, K. Observations on higher-order beam theory. *J. Aerosp. Eng. Proc. ASCE Tech. Note* **1993**, *6*, 408–413. [[CrossRef](#)]
7. Bickford, W.B. A consistent higher order beam theory. *Dev. Theor. Appl. Mech. SECTAM* **1982**, *11*, 137–150.
8. Ghugal, Y.M.; Sharma, R. A hyperbolic shear deformation theory for flexure and vibration of thick isotropic beams. *Int. J. Comput. Methods* **2009**, *6*, 585–604. [[CrossRef](#)]
9. Ghugal, Y.M.; Shimpi, R.P. A review of refined shear deformation theories for isotropic and anisotropic laminated beams. *J. Reinf. Plast. Compos.* **2002**, *21*, 775–813. [[CrossRef](#)]
10. Ghugal, Y.M. *A Simple Higher Order Theory for Beam with Transverse Shear and Transverse Normal Effect*; Department Report 4; Applied of Mechanics Department, Government College of Engineering; Aurangabad, India, 2006.
11. Heyliger, P.R.; Reddy, J.N. A higher order beam finite element for bending and vibration problems. *J. Sound Vib.* **1988**, *126*, 309–326. [[CrossRef](#)]
12. Ambartsumyan, S.A. On the theory of bending plates. *Izv Otd Tech Nauk AN SSSR* **1958**, *5*, 69–77.
13. Kruszewski, E.T. *Effect of Transverse Shear and Rotatory Inertia on the Natural Frequency of a Uniform Beam*; NACA-TN-1909; National Advisory Committee for Aeronautics: Washington, DC, USA, 1949.
14. Reddy, J. A general non-linear third order theory of plates with moderate thickness. *Int. J. Non-Linear Mech.* **1990**, *25*, 677–686. [[CrossRef](#)]
15. Touratier, M. An efficient standard plate theory. *Int. J. Eng. Sci.* **1991**, *29*, 901–916. [[CrossRef](#)]
16. Stein, M. Vibration of beams and plate strips with three-dimensional flexibility. *Trans. ASME J. Appl. Mech.* **1989**, *56*, 228–231. [[CrossRef](#)]
17. Soldatos, K.P. A transverse shear deformation theory for homogeneous monoclinic plates. *Acta Mech.* **1992**, *94*, 195–200. [[CrossRef](#)]
18. Karama, M.; Afaq, K.S.; Mistou, S. Mechanical behavior of laminated composite beam by new multi-layered laminated composite structures model with transverse shear stress continuity. *Int. J. Solids Struct.* **2003**, *40*, 1525–1546. [[CrossRef](#)]
19. Sayyad, A.S. Comparison of various refined beam theories for the bending and free vibration analysis of thick beams. *Appl. Comput. Mech.* **2011**, *5*, 217–230.
20. Sayyad, A.S. Comparison of various shear deformation theories for the free vibration of thick isotropic beams. *Int. J. Civ. Struct. Eng.* **2011**, *2*, 85–97.
21. Goldschmidtboeing, F.; Woias, P. Characterization of different beam shapes for piezoelectric energy harvesting. *J. Micromech. Microeng.* **2008**, *18*, 104013. [[CrossRef](#)]
22. Hildebrand, F.B.; Reissner, E.C. Distribution of stress in built-in beam of narrow rectangular cross section. *J. Appl. Mech.* **1942**, *64*, 109–116. [[CrossRef](#)]
23. Baroudi, S.; Najar, F.; Jemai, A. Static and dynamic analytical coupled field analysis of piezoelectric flexoelectric nanobeams: A strain gradient theory approach. *Int. J. Solid Struct.* **2018**, *153*, 110–124. [[CrossRef](#)]
24. Elshafei, M.A.; Alraies, F. Modeling and analysis of smart piezoelectric beams using simple higher order shear deformation theory. *Smart Mater. Struct.* **2013**, *22*, 035006. [[CrossRef](#)]
25. Hadjigeorgiou, E.P.; Stavroulakis, G.E.; Massalas, C.V. Shape control and damage identification of beams using piezoelectric actuation and genetic optimization. *Int. J. Eng. Sci.* **2006**, *44*, 409–421. [[CrossRef](#)]
26. Wang, Q.; Quek, S.T.; Sun, C.T.; Liu, X. Analysis of piezoelectric coupled circular plate. *Smart Mater. Struct.* **2001**, *10*, 229–239. [[CrossRef](#)]
27. Hadjigeorgiou, E.P.; Kalpakides, V.K.; Massalas, C.V. A general theory for elastic dielectrics. II. The variational approach. *Int. J. Non-Linear Mech.* **1999**, *34*, 967–980. [[CrossRef](#)]
28. Qirong, L.; Zhengxing, L.; Zhanli, J. A close-form solution to simply supported piezoelectric beams under uniform exterior pressure. *Appl. Math. Mech.* **2000**, *21*, 681–690. [[CrossRef](#)]
29. Fernandes, A.; Pouget, J. Accurate modeling of piezoelectric plates: Single-layered plate. *Arch. Appl. Mech.* **2001**, *71*, 509–524. [[CrossRef](#)]
30. Komeili, A.; Akbarzadeh, A.H.; Doroushi, A.; Eslami, M.R. Static Analysis of Functionally Graded Piezoelectric Beams under Thermo-Electro-Mechanical Loads. *Adv. Mech. Eng.* **2011**, *3*, 153731. [[CrossRef](#)]
31. Zhou, Y.; Chen, Y.; Ding, H. Analytical modelling and free vibration analysis of piezoelectric bimorphs. *J. Zhejiang Univ.-Sci. A* **2005**, *6*, 938–944. [[CrossRef](#)]
32. Thongchom, C.; Roodgar Saffari, P.; Roudgar Saffari, P.; Refahati, N.; Sirimontree, S.; Keawsawasvong, S.; Titotto, S. Dynamic response of fluid-conveying hybrid smart carbon nanotubes considering slip boundary conditions under a moving nanoparticle. *Mech. Adv. Mater. Struct.* **2022**, 1–14. [[CrossRef](#)]
33. Elaikh, T.E.; Abed, N.M.; Ebrahimi-Mamaghani, A. Free vibration and flutter stability of interconnected double graded micro pipes system conveying fluid. *IOP Conf. Ser. Mater. Sci. Eng.* **2020**, *928*, 022128. [[CrossRef](#)]

Disclaimer/Publisher's Note: The statements, opinions and data contained in all publications are solely those of the individual author(s) and contributor(s) and not of MDPI and/or the editor(s). MDPI and/or the editor(s) disclaim responsibility for any injury to people or property resulting from any ideas, methods, instructions or products referred to in the content.